ORNL/TM-2000/270

Metals and Ceramics Division

Fatigue Properties of Type 316LN Stainless Steel as a Function of Frequency and Waveform

J. P. Strizak and J. R. DiStefano

Date Published: October 2000

Prepared for the
U. S. Department of Energy
Spallation Neutron Source

Prepared by the
OAK RIDGE NATIONAL LABORATORY
Oak Ridge, Tennessee 37831-6285
operated by
UT-Battelle, LLC
for the
U.S. DEPARTMENT OF ENERGY
under contract DE-AC05-00OR22725

CONTENTS

FIGURES

Figure **Page**

TABLES

ABSTRACT

The low cycle fatigue behavior of type 316LN stainless steel was investigated in air and mercury at frequencies from 0.1 to 10 Hz. Cyclic stress ratios (R) of -1 and 0.1 were used with sinusoidal, triangular and positive sawtooth wave forms. Mercury appears to reduce fatigue life at high stress amplitudes, but the endurance limit may be unaffected. Low frequency and mean stress decreased the fatigue endurance limit, but type of waveform did not appear to affect fatigue life under the conditions of these tests.

1. INTRODUCTION

The target material for the Spallation Neutron Source (SNS) will be liquid mercury that is contained within a type 316LN stainless steel vessel. The mercury target container will be subjected to a variety of loading conditions in this application, and structural design criteria for the target system have been developed which require a consideration of cyclic stresses during service.[1] In support of the data needs an experimental program is underway to determine the fatigue properties of type 316LN stainless steel in air and mercury[2] in both high and low cycle regimes. Previously,[2] screening tests conducted in air and mercury using a sinusoidal wave form with R ratio (minimum stress/maximum stress), of -1 had indicated a reduction (2 – 3X) in fatigue life in mercury at high stress amplitudes. Furthermore, examination of the fractures in mercury revealed secondary cracking and little evidence of ductility. If mercury wets the freshly cracked surfaces during fatigue testing and crack growth rate is accelerated as a result of this interaction (e.g., liquid metal embrittlement), such effects could be exacerbated by waveforms such as positive saw-tooth, i.e., slower rate to achieve maximum stress amplitude followed by faster reverse rate. In order to evaluate effects of load application on fatigue behavior, a series of tests has been conducted to evaluate sinusoidal wave, triangular wave and positive sawtooth types of load on fatigue properties at several low frequencies.

2. EXPERIMENTAL

A single heat of mill-annealed type 316LN stainless steel material was used for the fatigue tests. The 25-mm thick plate from which the specimens were machined met the American Society for Testing and Materials (ASTM) specification A240-88C, and the composition and relevant physical and mechanical properties of this material are shown in Table 1. Additional information regarding the general microstructure, tensile properties, and strain-controlled low-cycle fatigue properties is recorded elsewhere.[3]

Table 1. Vendor ladle analysis for Jessop Steel Company heat 18474 type 316LN stainless steel. Selected physical and mechanical properties for the mill annealed material also included.

Element	Weight percent
C	0.009
Mn	1.75
P	0.029
S	0.002
Si	0.39
Ni	10.2
Cr	16.31
Mo	2.07
Co	0.16
Cu	0.23
N	0.11
Fe	Balance
Room temperature properties (test at strain rate 8×10^{-5}/s)	
0.2% offset yield strength	259.1 MPa
Ultimate tensile strength	587.5 MPa
Elongation	86.2%
Reduction of area	88.1%
Grain size	ASTM 3.7

Fatigue test specimens (see Fig. 1) were machined parallel to the primary rolling direction of the 25-mm plate. To hold Hg around the gage section of the specimen during testing, press-fit bushings fabricated from commercially pure nickel and aluminum were designed to fit the ends of the fatigue specimens. Figure 2 shows the bushing design that comprises the primary mercury containment system. The bushing

(vile) on the lower half of the specimen extends from the extreme bottom to just above the top end of the gage section, forming a cup around the gage section. The top end of the specimen was fitted with an aluminum bushing with the same outside diameter as the lower half to facilitate gripping in the fatigue machine. The entire assembly was loaded into the fatigue machine surrounded by a large plastic bag to contain any mercury that might tend to be dislodged from the cup as the specimen fractured.

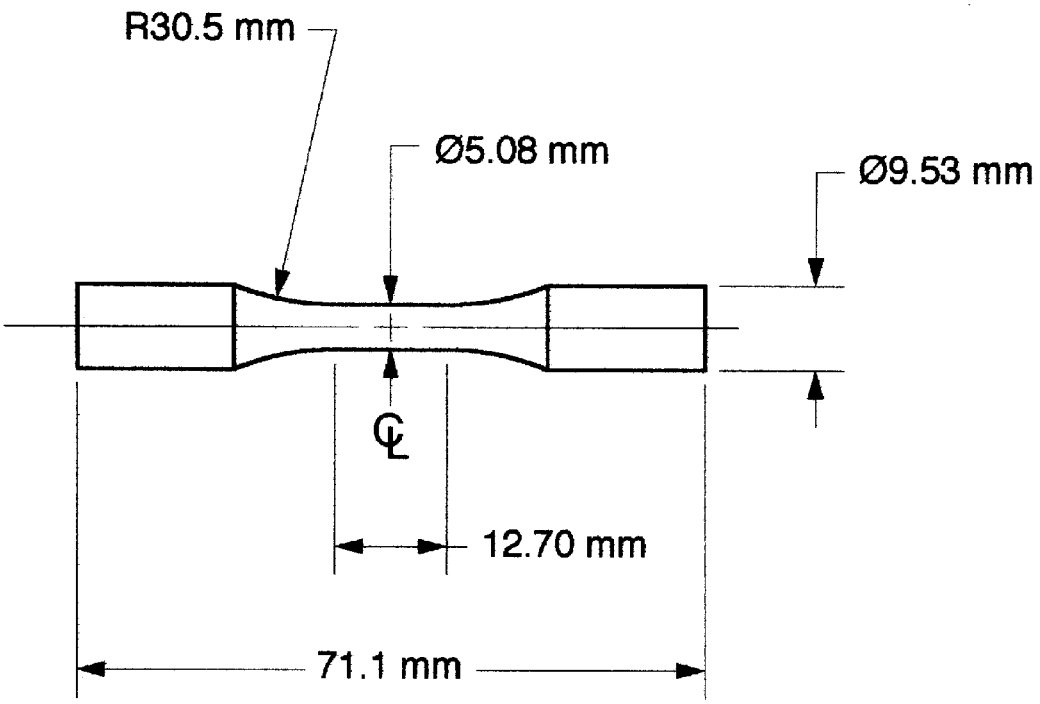

Fig. 1. Type of fatigue specimen used in this study.

The uniaxial load controlled fatigue tests were performed with fully reversed loading (R = -1, compressive minimum stress/tensile maximum stress) or R = 0.1 (mean tensile stress). The loading frequency was varied from 1 to 10 Hz. The test procedure, including due consideration for specimen alignment, followed ASTM E606.[4]

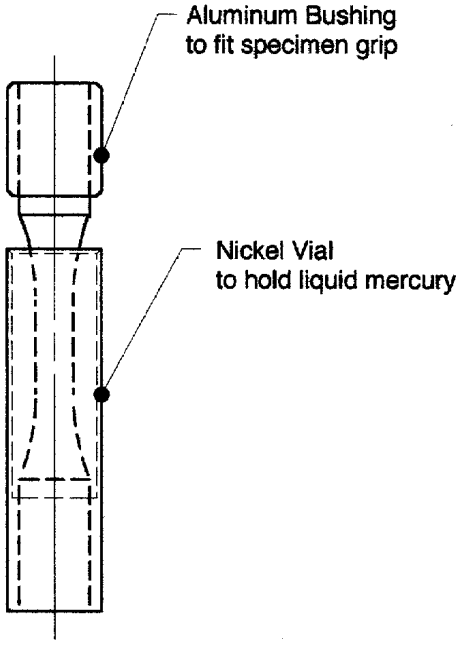

Fig. 2. Fatigue specimen with bushing and vial for containment of mercury.

3. RESULTS AND DISCUSSION

Before presenting the specific results generated in this study, it would be useful to review how the fatigue or endurance limit, which represents the stress level below which the material will not fail due to cyclic loading, is determined.

First, it should be noted that the relation between alternating stress that defines endurance limit (S) and cycles to failure (N_f) is not necessarily an absolute value function, but it does indicate a probabilistic tendency. In terms of the parameters that are used in fatigue testing,

Stress ratio: $R = \frac{\sigma_{min}}{\sigma_{max}}$

Stress range: $\Delta\sigma_r = \sigma_{max} - \sigma_{min}$

Alternating stress: $\sigma_a = \frac{\sigma_{max} - \sigma_{min}}{2}$

Mean stress: $\sigma_m = \frac{\sigma_{max} + \sigma_{min}}{2}$

Thus, for the same σ_{max}, the values for the above parameters change with σ_{min}. The data in the present study was obtained at R = -1 and R = 0.1. For R = -1, $\sigma_a = \sigma_{max}$ and $\sigma_m = 0$. For R = 0.1, $\sigma_a = .45\ \sigma_{max}$ ($\sigma_{max} = 2.22\ \sigma_a$) and $\sigma_{mean} = .55\ \sigma_{max}$. A schematic plot of σ_a (alternating stress) versus mean stress is shown in Fig. 3. In this graph the limiting value of σ_a is taken to be σ_f, the true stress at fracture. At $\sigma_m = 0$, (R = -1), the highest possible value for σ_a is σ_f. For well behaved materials it should also be true that $\sigma_a + \sigma_m = \sigma_f$, i.e., for a given stress level, σ_{max}, the value of σ_a decreases linearly with increasing mean stress as shown in Fig. 3. This type of behavior is usually valid if the plastic strain damage produced each cycle is independent and not cumulative. Empirical relations have been developed as well, and three such examples based on linear or parabolic effects of mean stress that varies from 0 to the yield or ultimate stress are indicated schematically in Fig. 4. Experimentally, it has been found that a majority of data for ductile metals fall between the lines representing the Gerber and Goodman empirical relationships.[5]

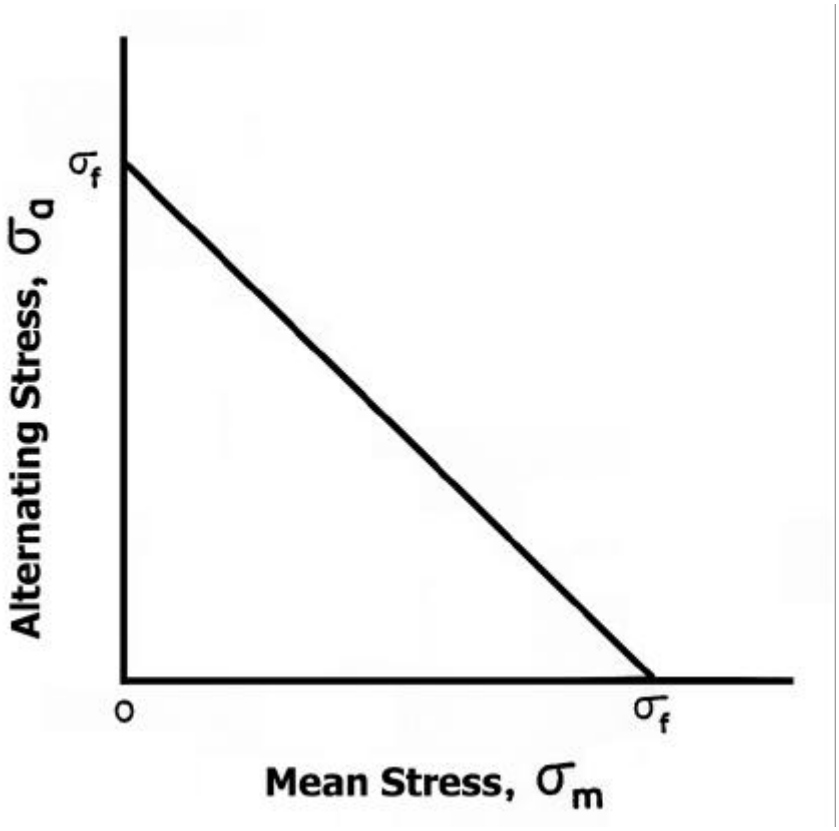

Fig. 3. Generalized effect of mean stress on fatigue endurance limit.

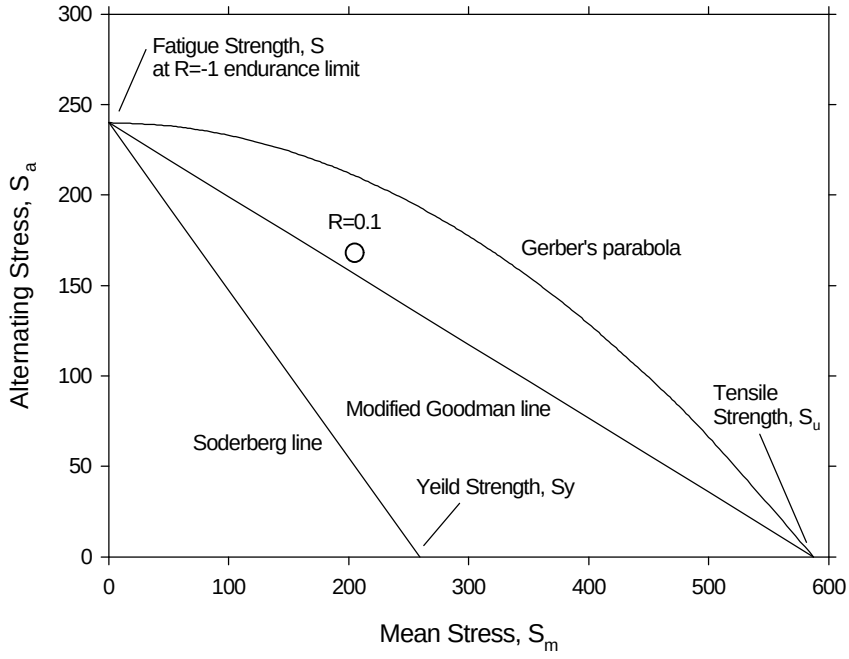

Fig. 4. Empirical diagrams showing effect of mean stress on fatigue endurance limit.

The above discussion refers to fatigue under conditions of constant amplitude and constant frequency. When components are subject to fluctuating loading conditions, mean stresses, and variable frequencies, more complicated damage theories must be applied.

3.1 Effect of Mercury

Figures 5 and 6 show results for 316LN at different frequencies in both air and mercury for R = -1 or 0.1, respectively. For R = -1 at high stress amplitudes, mercury appears to reduce fatigue life by a factor of 2 – 3X while the endurance limit appears to be converging at approximately 230-240 MPa. For R = 0.1 (mean stress), however, the data appear to converge at approximately 160-170 MPa (Fig. 6).

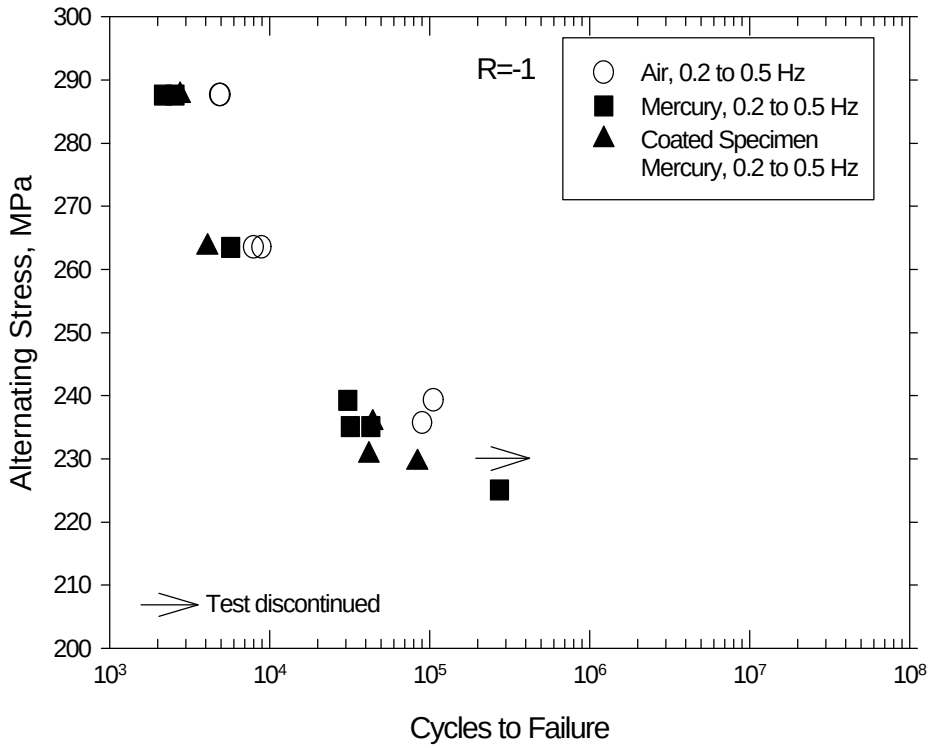

Fig. 5. Fatigue data for 316LN stainless steel in air and mercury for R = -1.

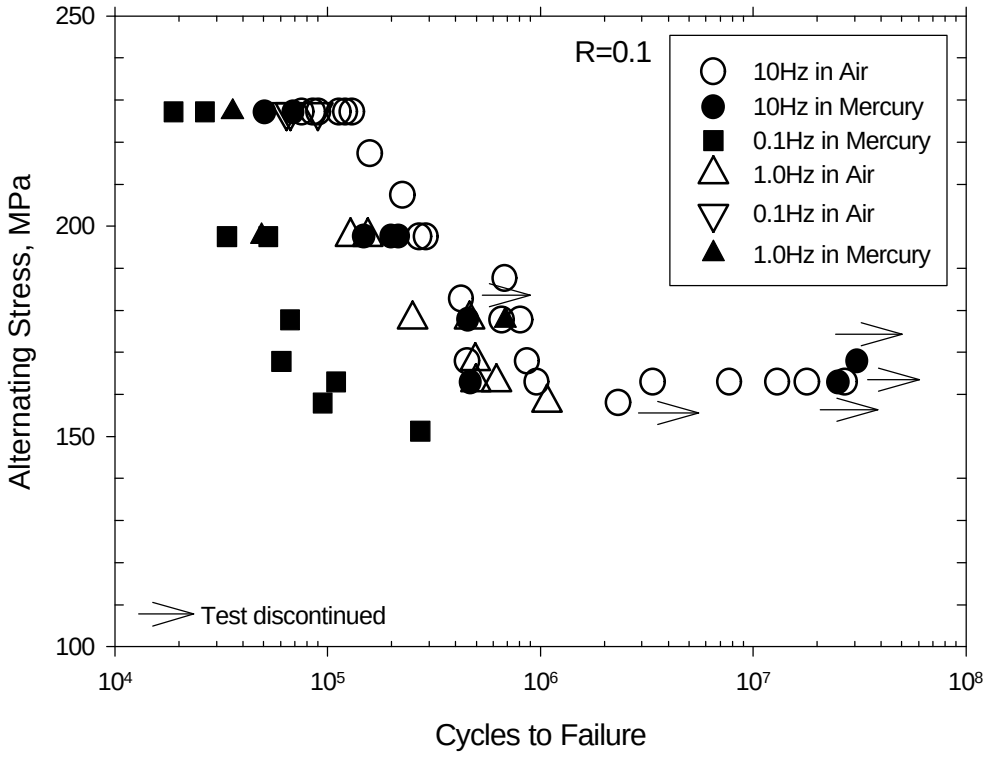

Fig. 6. Fatigue data for 316LN stainless steel in air and mercury for R = 0.1.

3.2 Effect of Frequency

For R = 0.1, the data in air and mercury are plotted separately in Figs. 7 and 8, respectively, to better differentiate the effect of frequency. Shorter fatigue lives are associated with lower frequencies in both environments; however, the frequency effect was greater in mercury where the fatigue life at 0.1 Hz was up to 10X lower than at 1 and 10 Hz (Fig. 8). These data also suggest some effect of frequency on endurance limit. In fatigue crack growth tests in air, it was previously observed[6] that at frequencies in the ranges 0.0067 Hz to 6.67 Hz at 538°C, crack growth rate increased as the frequency decreased. Since wetting by mercury is likely to be enhanced in a freshly formed crack, it might be expected that LME effects would result in a more significant frequency effect in mercury compared with air. However, between 10-700 Hz no significant effect of frequency was found in a comparison study[7] when test temperature at high frequency was controlled. Thus, frequency effects may disappear between 1 and 10 Hz.

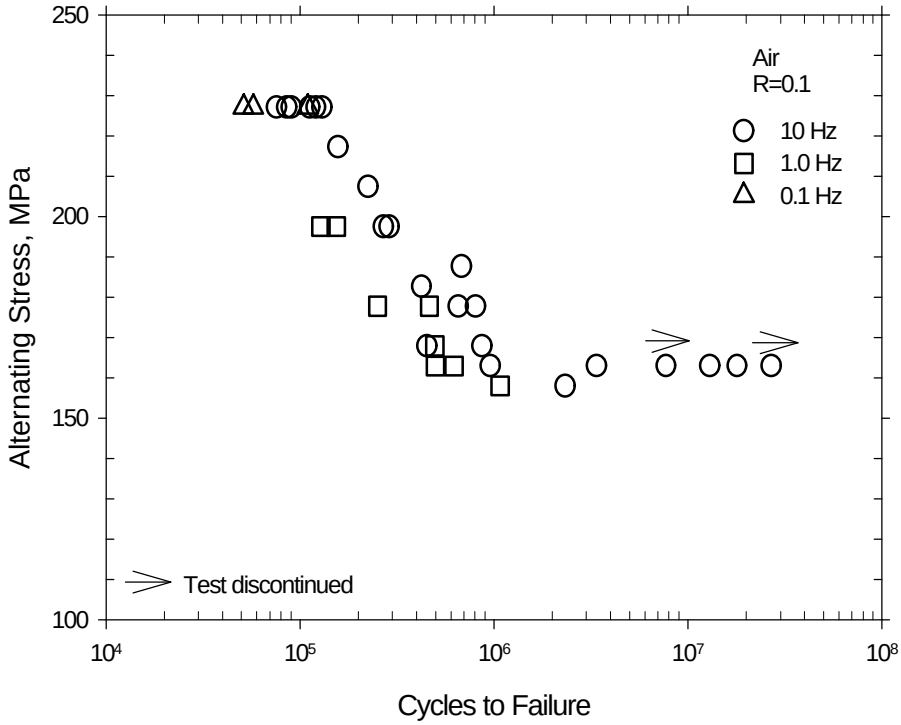

Fig. 7. Effect of frequency on fatigue life of 316LN stainless steel in air for R = 0.1.

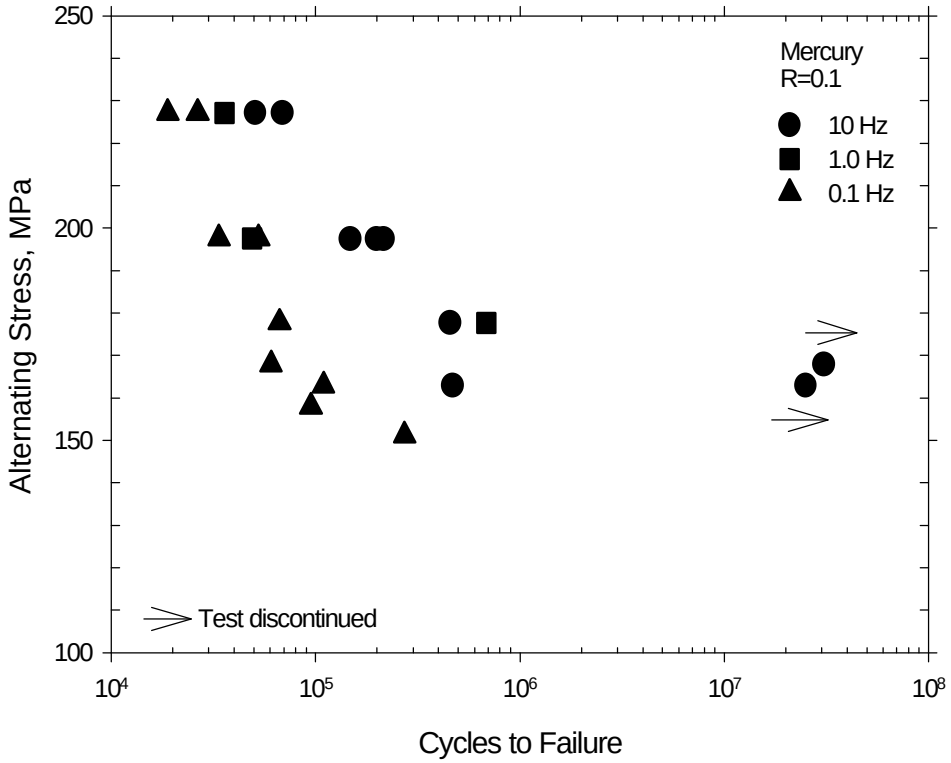

Fig. 8. Effect of frequency on fatigue life of 316LN stainless steel in mercury for R = 0.1.

3.3 Effect of Mean Stress

Comparison of the data in Fig. 5 (R = -1) with that in Fig. 6 (R = 0.1) shows that mean stress lowers the fatigue life for equivalent values of stress amplitude, and, thus lowers the endurance limit, S. At R = -1, an endurance limit of approximately 230-240 MPa is projected, but S drops to approximately 160-170 MPa at R = 0.1. However, as described above, when R = -1, $\sigma_{mean} = 0$ and $\sigma_{max} = S$, but when R = 0.1, $\sigma_{mean} = 0.1\ \sigma_{max}$ and $\sigma_{max} = S/0.45$. Figure 4 shows the endurance limits from this study for R = -1 (no mean stress) and R = 0.1 (mean stress). Note that at R = 0.1, the endurance limit decreased as a result of the mean stress and lies between the Modified Goodman and Gerber predictions as was expected.

3.4 Effect of Waveform

In general, once a crack forms in a fatigue test there is a critical stress threshold σ_{th}, required for the crack to propagate. At a constant frequency and $\sigma_{max} \geq \sigma_{th}$, the time per cycle the specimen is stressed above σ_{th} while the crack is opening depends upon the shape of the wave. For example if $\sigma_{th} = .75\ \sigma_{max}$, the positive sawtooth waveform has the highest crack-opening time with the sinusoidal and triangular waveforms being significantly lower. This type of effect can be exacerbated by an environment that also enhances crack growth.

Figure 9 summarizes the effects of cyclic loading waveform on fatigue life. At 10 Hz, waveform (sinusoidal vs triangular) did not significantly affect fatigue life in air. At 0.1 Hz, results were also similar when sinusoidal, triangular or positive sawtooth waveforms were used. Results in mercury were less consistent. At 10 Hz, the sinusoidal waveform resulted in a longer fatigue life compared with triangular, but at 0.1 Hz, fatigue life was longer for the triangular waveform. It can also be noted that with a triangular waveform, reducing the frequency from 10 to 0.1 Hz decreased the fatigue life to a lesser extent than observed for the sinusoidal waveform. Environmental effects on fatigue life and fatigue crack growth rate involve a complex interaction of a number of variables including environmental embrittlement, mean stress, stress intensity at the crack tip, temperature, stress-time dependence, etc. Considering stress-time dependence, differences in the frequency effects in mercury may be partially related to the shorter time that the triangular waveform subjects the crack tip to some critical stress threshold compared with the sinusoidal waveform.

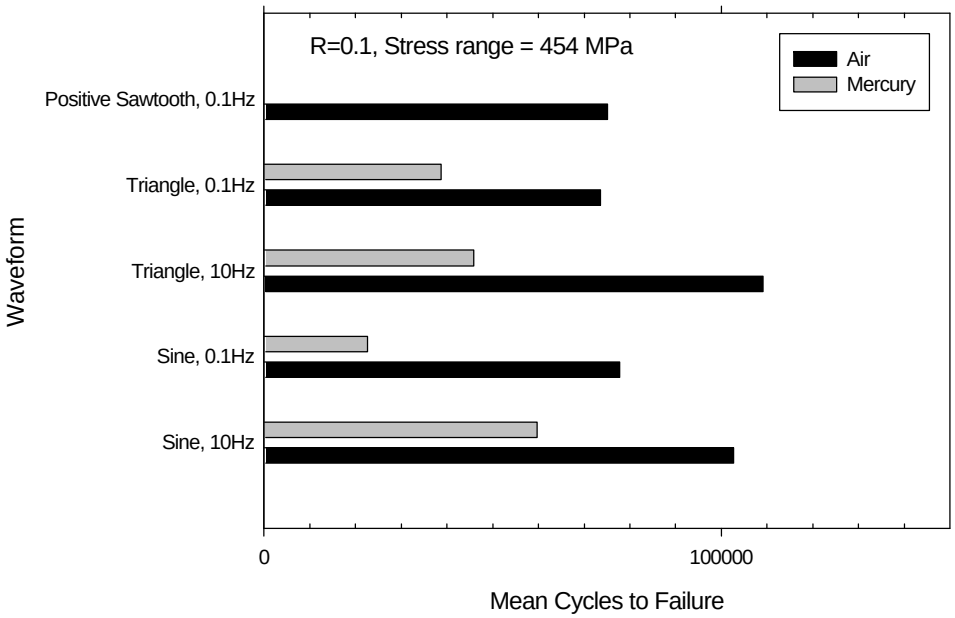

Fig. 9. Bar graph comparison of the effect of waveform on fatigue life in air and mercury.

4. CONCLUSIONS

Fatigue design data have been developed for type 316LN stainless steel to be used for containment of the mercury target of the SNS. Results thus far indicate that:

1. At high stress amplitudes mercury reduces the fatigue life, but the endurance limit does not appear significantly different than in air.
2. Low frequencies, i.e., below approximately 10 Hz, reduce the fatigue life in both air and mercury. Reduction was somewhat greater in mercury. No effect of mercury was found at frequencies from 10 Hz to 700 Hz.
3. Mean stress (R = 0.1) reduces the fatigue life in both air and mercury. The reduction found in this study falls between that predicted by Gerber's parabola and the modified Goodman line.
4. Type of waveform did not significantly affect fatigue under the conditions used in this study.

ACKNOWLEDGMENTS

The authors would like to acknowledge the helpful role of may individuals. E. T. Manneschmidt contributed to fabrication of specimens tested in mercury and R. L. Martin operated the fatigue testing machines. R. B. Ogle and S. N. Lewis provided advice on Industrial Hygiene and services for controlling mercury exposures. S. J. Pawel provided critical review of the manuscript. F. C. Stooksbury and K. A. Choudhury prepared the manuscript and figures.

REFERENCES

1. G. T. Yahr and C. R. Luttrell, *Title I Structural Design Criteria for SNS Target Module*, SNS/TSR-181, April 5, 2000.

2. S. J. Pawel, J. R.DiStefano, J. P. Strizak, C. O. Stevens, and E. T. Manneschmidt, *Screening Test Results of Fatigue Properties of Type 316LN Stainless Steel in Mercury*, ORNL/TM-13759 (SNS/TSR-0097), March 1999.

3. R. W. Swindeman, *HWR-NPR Materials/Systems Integrity Mechanical Behavior Report*, ORNL/NPR-92/94, Martin-Marietta Energy Systems, Incorporated, Oak Ridge National Laboratory, June 1993.

4. ASTM Standard E606, "Standard Recommended Practice for Constant-Amplitude Low-Cycle Fatigue Testing," *Annual Book of ASTM Standards*, Vol. 03.01, 1992.

5. Marc André Meyers and Krishan Kumar Chowla, *Mechanical Metallurgy, Principles and Applications*, Prentice-Hall, Incorporated, Englewood Cliffs, NJ 07632, p. 700.

6. J. E. Campbell, "Fracture Properties of Wrought Stainless Steels," in *Application of Fracture Mechanics for Selection of Metallic Structural Materials*, J. E. Campbell, W. W. Gerberich, and J. H. Underwood, Eds., American Society for Metals, Metals Park, OH, 1982, p. 131.

7. H. Tian, et al., "Influence of Mercury Environment on Fatigue Behavior of Spallation Neutron Source (SNS) Target-Container Materials," submitted to Materials Science and Engineering for honoring Professor Campbell Laird, 2000 TMS Annual Meeting, Nashville, TN, March 12-16.

INTERNAL DISTRIBUTION

1. R. R. Allen
2. R. E. Battle
3. E. E. Bloom
4. K. K. Chipley
5. J. E. Cleaves
6. J. W. Cobb
7. H. H. Cromwell
8. J. H. DeVan
9-13. J. R. DiStefano
14. D. A. Everitt
15. K. Farrell
16. T. A. Gabriel
17. J. R. Haines
18. L. L. Horton
19. J. D. Hunn
20. L. L. Jacobs
21. D. R. Johnson
22. J. O. Johnson
23. A. G. Jordan
24. E. H. Lee
25. D. C. Lousteau
26. A. T. Lucas
27. E. T. Manneschmidt
28. L. K. Mansur
29. T. E. Mason
30. T. J. McManamy
31. G. E. Michaels
32. D. E. Moncton
33. A. E. Pasto
34-38. S. J. Pawel
39. M. J. Rennich
40. S. L. Schrock
41. P. T. Spampinato
42. C. N. Strawbridge
43. J. P. Strizak
44. R. P. Taleyarkhan
45. P. T. Tortorelli
46. J. H. Whealton
47. D. K. Wilfert
48. G. T. Yahr
49. G. L. Yoder
50-51. Central Research Library
52. Document Reference Section
53-54. ORNL Laboratory Records–RC
55. Office of Scientific & Technical Information

EXTERNAL DISTRIBUTION

56. G. Bauer, Paul Scherrer Institute, CH-5232, Villigen-PSI, Switzerland

57. J. M. Carpenter, Argonne National Laboratory, 9700 South Cass Avenue, Building 360, IPNS Division, Argonne, IL 60439

58. A. Jason, Los Alamos National Laboratory, P.O. Box 1663, H817 LANSCE-1, Los Alamos, NM 87545

59. P. Liaw, University of Tennessee, Department of Materials Science & Engineering, 427-B Dougherty Building, Knoxville, TN 37996-2200

60. W. Sommer, Los Alamos National Laboratory, P.O. Box 1663, Lansce-2, Los Alamos, NM 87545

61. M. Todosow, Brookhaven National Laboratory, P.O. Box 5000, Building 475B, Upton, NY 11973

62. M. Wechsler, 106 Hunter Hill Place, Chapel Hill, NC 27514-9128

63. W. Weng, Brookhaven National Laboratory, P.O. Box 5000, Building 911B, Upton, NY 11973